The design of energy storage based on thermoelectric generator and bidirectional converter

Razman Ayop[1], Chee Wei Tan[1], Abba Lawan Bukar[2], Awang Jusoh[1], Nik Din Muhamad[1], Syed Norazizul Syed Nasir[1]
[1]School of Electrical Engineering, Faculty of Engineering, Universiti Teknologi Malaysia, Johor Bahru, Malaysia
[2]Department of Electrical and Electronic Engineering, University of Maiduguri, Maiduguri, Nigeria

Article Info

Article history:

Received Apr 21, 2022
Revised Jun 6, 2022
Accepted Jun 21, 2022

Keywords:

Maximum power point
P&O
Peltier device
Perturb and observe method
Thermoelectric generator

ABSTRACT

Energy storage plays an important role in the future of the power system. There are a lot of energy storage system (ESS) available and thermal energy storage shows a promising future. Conventionally, this system is based on a steam generator that converts heat energy to electrical energy and an electrical heater to convert electrical energy to heat energy. Nonetheless, there is still no proper ESS based on the thermoelectric generator (TEG), which can convert directly heat energy to electrical energy and vice versa. This paper proposed a power converter with a new controller for the thermal ESS based on the TEG. The bidirectional converter and the modified perturb and observe method are used to manage the energy transfer at the TEG. The thermal energy storage is based on the sensible approach, where the heat energy causes the temperature to increase. The results show that the thermal ESS based on the TEG is feasible since the energy can be stored and released from the proposed system.

Corresponding Author:

Razman Ayop
School of Electrical Engineering, Faculty of Engineering, Universiti Teknologi Malaysia
81310 Johor Bahru, Johor, Malaysia
Email: razman.ayop@utm.my

1. INTRODUCTION

Energy storage has an important role especially today since now we are transitioning toward renewable energy. This is because renewable energy such as solar and wind energy has an intermediate characteristic. This allows the excess energy produced by renewable energy to be used when the energy production is low. According to Renewables 2021 Global Status Report (GSR), there has been a 139 GW and 93 GW increase in energy produced by the solar photovoltaics (PV) and wind turbine, respectively [1]. This is proof that the energy storage technology needs to catch up with this renewable energy.

There are various energy storage technologies used with the renewable energy system [2]-[4]. The top ten countries by installed capacity of the energy storage show that mechanical energy storage such as pumped hydro [5], compressed air [6], and flywheel [7] is the commonly chosen. This is due to the large energy storage capability. However, pumped hydro has location constraints and can impact the environment. While compressed air has leakage problems and safety issues. The flywheel also has noise problems and is high in cost. The battery is also an option to store the energy [8]. The lithium-ion battery has high-energy, high-power density, and fast response time. However, the cost is high and the life cycle depends on the discharge level. The lead-acid battery is lower in cost but has low energy and power density.

Thermal energy storage stores the energy in the form of heat in the material such as the ground, water, or phase change materials. The thermal energy storage for 2017 is near 3.3 GW and it is expected to increase up to 11% from 2017 to 2022, which shows that the energy storage in the form of heat has the potential [2]-[4]. The thermoelectric generator (TEG), can convert the heat energy to electrical energy and electrical energy to heat energy directly without any additional energy conversion. Therefore, the TEG has the potential to be used as energy storage, in which the energy is stored in the form of heat. Commonly, the TEG is used in the heat energy recovery application such as in industries likes the sugar factory [9] or automotive industry [10]. It is also being used in energy generation based on solar thermal and photovoltaic energies [11], [12]. However, the TEG energy storage system (ESS) is still in the early phase. The current research focuses more toward the TEG and the heat storage material rather than the power converter and the controller used to integrate the TEG into the grid, as described in Figure 1 [13]-[15]. Based on the research, the TEG is either open-circuited or manually controlled using the power supply and load, which is not realistic if the TEG is connected to a grid. Therefore, a specially designed power converter with an optimized controller is needed for the TEG based ESS.

This paper proposed the integration of a power converter for the ESS based on the TEG array. The bidirectional converter is used to store and supply energy from or to the DC bus. A control strategy based on the maximum power point (MPPT) perturb and observe (P&O), the method is proposed to control the bidirectional converter. The next section discusses the design of an ESS based on TEG. The third section provides the results and discussions on the proposed system. The last section concludes the finding of the research.

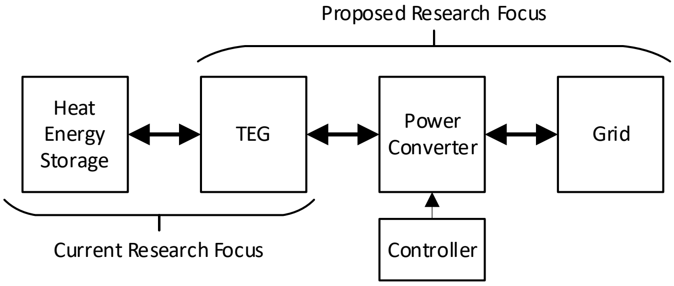

Figure 1. The current trend and the proposed research on TEG ESS

2. DESIGN OF ENERGY STORAGE SYSTEM BASED ON THERMOELECTRIC GENERATOR

The block diagram of the ESS based on the TEG array and bidirectional converter is shown in Figure 2. The TEG array consists of 2 sides, the hot and cold sides. The cold site is exposed to the environment. A heat sink is added to increase the surface area for the heat exchange to happen between the TEG and the environment. The low temperature, T_l, is kept constant at 30 °C similar to the environment. The hot side of the TEG array is connected to a heat energy storage, which has a high temperature, T_h. The TEG array is connected to the bidirectional converter.

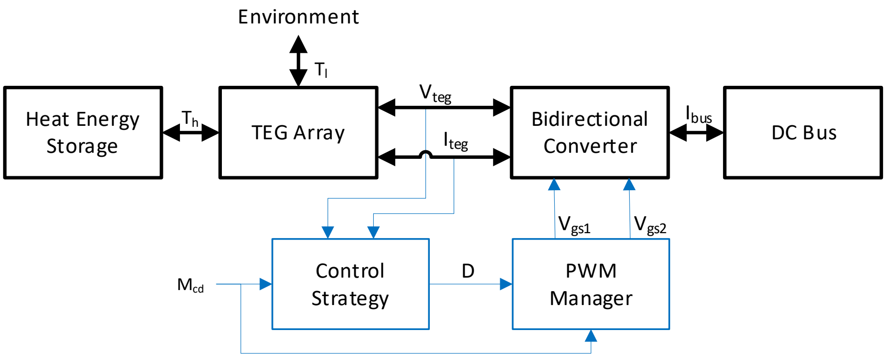

Figure 2. The block diagram of the ESS based on the TEG array and bidirectional converter

The TEG voltage and current (V_{teg} and I_{teg}, respectively) are measured and sent to the control strategy. Depending on the mode charge/discharge, M_{cd}, an appropriate control strategy determines the duty cycle, D, for the bidirectional converter. The pulse width modulation (PWM) manager uses the D and M_{cd} to produce an appropriate gate-source voltage 1 and 2 (V_{gs1} and V_{gs2}, respectively). The V_{gs1} and V_{gs2} drive the bidirectional converter to absorb or supply the power from or to the DC bus. This is observed by analysing the bus voltage and current, V_{bus} and I_{bus}, respectively.

2.1. Thermoelectric generator model

The TEG array consists of only two components, which are the voltage source and the resistor [16], [17]. The voltage source has the magnitude of internal voltage, V_{int}, which is calculated using (1). The resistor has the value of internal resistance, R_{int}, which is calculated using (2). These two components are connected in series. Since this is the TEG array, the number of TEG modules connected in series and parallel, N_{ser} and N_{par}, respectively, are included in the TEG model. The Seebeck coefficient of a unit of TEG module, S_{tegu}, and the temperature difference, $\Delta T = T_h - T_l$, affect the V_{int}. The internal resistance of a unit TEG module, R_{intu}, is obtained from the TEG module datasheet.

$$V_{int} = N_{ser} S_{tegu} \Delta T \quad (1)$$

$$R_{int} = \frac{N_{ser}}{N_{par}} R_{intu} \quad (2)$$

The electrical modelling of the TEG arrays only involves (1) and (2). Since the heat energy involves in the proposed system, the modelling of the heat energy part of the TEG array needs to be considered. The heat power generated at the low and high-temperature sides of the TEG array (Q_l and Q_h, respectively) is calculated using (3) and (4) [16]. In the model, the thermal conductance, K_{tc}, are considered. While the power generated by the electrical part of the TEG, W_{teg}, is calculated using (5). The relationship between the Q_l, Q_h, W_{teg}, and heat energy that goes into heat energy storage, Q_m, is shown in (6).

$$Q_l = S_{tegu} T_l I_{teg} - 0.5 {I_{teg}}^2 R_{int} + K_{tc}(T_l - T_h) \quad (3)$$

$$Q_h = -S_{tegu} T_h I_{teg} - 0.5 {I_{teg}}^2 R_{int} + K_{tc}(T_h - T_l) \quad (4)$$

$$W_{teg} = V_{teg} I_{teg} \quad (5)$$

$$Q_m = W_{teg} + Q_l + Q_h \quad (6)$$

2.2. Bidirectional converter

The non-galvanic isolated bidirectional converter is used for the ESS based on the TEG array, as shown in Figure 3(a). This converter is chosen due to its simplicity and low number of components. It requires 3 inductors, 2 capacitors, 2 diodes, and 2 MOSFETs. The name of the components is input inductance (L_i), input capacitance (C_i), middle inductance (L_m), MOSFET 1 (Q_1), diode 1 (D_1), MOSFET 2 (Q_2), diode 2 (D_2), output capacitance (C_o), and output inductance (L_o). The L_i and C_i filter the I_{teg} and V_{teg} and ensure the current and voltage ripple are acceptable. The L_o and C_o filter the I_{bus} to ensure the current ripple is acceptable. The L_m needs to be designed properly to ensure continuous current mode operation.

This converter operates in two modes, buck and boost modes [18], [19]. In buck mode, the energy flows from the DC bus to the TEG array. This is considered a charging mode. By referring to the PWM manager in Figure 3(b), the V_{gs1} becomes 0V and the MOSFET Q_1 becomes an open circuit. The output of the PWM is connected to the V_{gs2}. In boost mode, the energy flows from the TEG array to the DC bus. This is considered as discharging mode. The V_{gs2} becomes 0V and the MOSFET Q_2 becomes an open circuit. The output of the PWM is connected to the V_{gs1}.

The range of D for the bidirectional converter is between zero to one. However, due to the nonideality of the components inside the bidirectional converter, the D is kept to between 0 to 0.8 to avoid problems during the operation [20]. Since the D highly depends on the V_{teg} and V_{bus}, a proper configuration of the TEG array and suitable V_{bus} need to be done. The relationship between D, V_{teg}, and V_{bus} is shown in (7) and (8), which is based on the conventional buck and boost converters [20]. The charge D, D_{ch}, is the operation based on the buck converter. While the discharge D, D_{disch}, is based on the boost converter. Note that the V_{bus} is constant during the operation.

In (9) is derived using (7), in which the V_{teg} is obtained using Kirchhoff voltage law. To avoid damage to the TEG array, the maximum V_{int} and I_{teg} ($V_{int(max)}$ and $I_{teg(max)}$, respectively) need to be set based on the manufacture datasheet of the TEG array. Based on this relationship, the maximum D_{ch}, $D_{ch(max)}$, is calculated. During discharge, the V_{teg} becomes half of the V_{int} [21], [22]. By implementing this condition into (8), (10) is obtained. To determine the maximum D_{disch}, $D_{disch(max)}$, the minimum V_{int}, $V_{int(min)}$, needs to be calculated by determining the minimum ΔT. Note that the derived (9) and (10) are based on an ideal bidirectional converter. The D for a practical bidirectional converter is higher when compared to the calculation. Therefore, the $D_{ch(max)}$ and $D_{disch(max)}$ needs to be lower than 0.8 to avoid problem during the operation. The design of the inductance and capacitance is complicated, which involves a complex mathematical analysis. Therefore, these parameters are designed using the try and error method.

$$D_{ch} = \frac{V_{teg}}{V_{bus}} \tag{7}$$

$$D_{disch} = 1 - \frac{V_{teg}}{V_{bus}} \tag{8}$$

$$\frac{V_{int(max)} + I_{teg(max)}R_{int}}{V_{bus}} \leq D_{ch(max)} \tag{9}$$

$$1 - \frac{V_{int(min)}}{2V_{bus}} \leq D_{disch(max)} \tag{10}$$

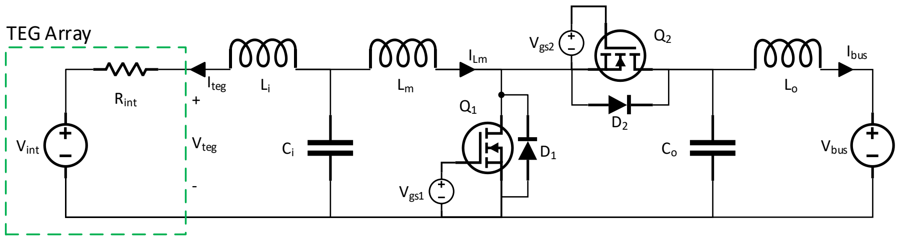

(a)

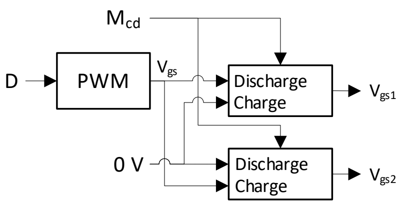

(b)

Figure 3. The equivalent circuit of the ESS based on the TEG array and bidirectional converter connected to the DC bus for (a) the main equivalent circuit and (b) the block diagram of the PWM manager

2.3. Proposed control strategy

The control strategy is based on the P&O MPPT algorithm since the TEG I-V characteristic curve is not linear with maximum power point [23], [24]. The control strategy determines the D needed to charge and discharge the system. By referring to Figure 4(a), the control strategy starts by measuring the V_{teg} and I_{teg}. The TEG power, P_{teg}, is calculated by multiplying the V_{teg} with the I_{teg}. The next step is based on the M_{cd}. If M_{cd} is "charge", the operation continues with Figure 4(b). If M_{cd} is "discharge", the operation continues with Figure 4(c). If M_{cd} is not "charge" or "discharge", the operation ended.

If the bidirectional converter operates in charging mode, the P_{teg} is compared with the reference power, P_{ref}. If the P_{ref} is less than P_{teg}, the previous D, D_0, is added with the duty cycle step size, D_{step}, to become the new D. Else, the D_0 is subtracted with the D_{step}. This ensures only certain power can charge the system, thus avoiding damaging the TEG array.

If the bidirectional converter operates in discharging mode, the P&O MPPT method is used [25], [26]. This is because the I-V characteristic of the TEG is nonlinear. The maximum power is produced when the load is equal to R_{int}. Since the bidirectional converter becomes the load of the TEG array, the input of the bidirectional converter is adjusted to match the R_{int} using P&O MPPT method [21], [27]. The operation starts by comparing the V_{teg} and P_{teg} with the previous V_{teg} and P_{teg} (V_{teg0} and P_{teg0}, respectively). Then the change of V_{teg} and P_{teg} (dV_{teg} and dP_{teg}, respectively) is multiplied together to become the product of change of V_{teg} and P_{teg}, dPV_{teg}. If the dPV_{teg} is less than zero, the D_0 is added with the D_{step}. Else, the D_0 is subtracted with the D_{step}.

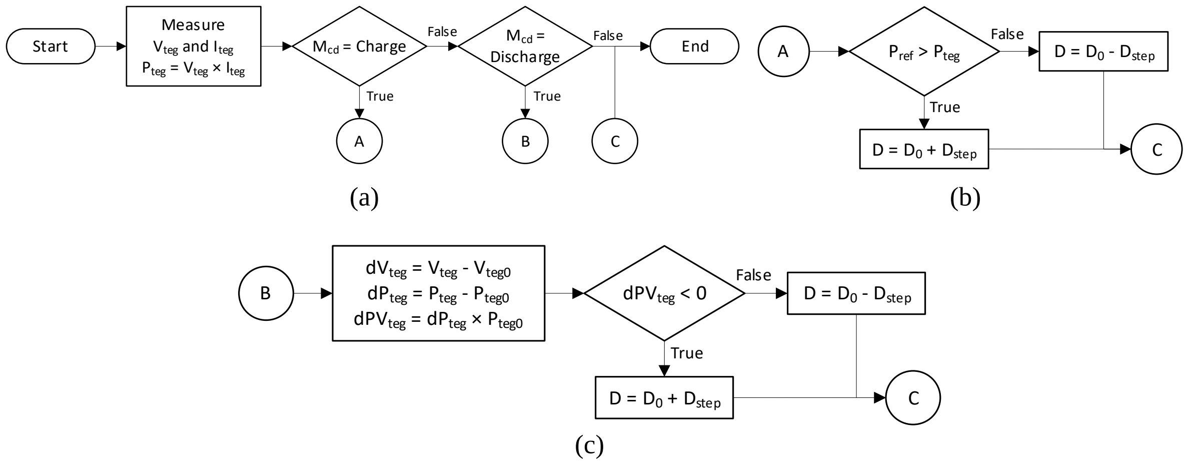

Figure 4. The flowchart of the control strategy using the P&O MPPT method for the ESS based on the TEG array and bidirectional converter for (a) the main control strategy, (b) the charging control strategy, and (c) the discharging control strategy

2.4. Heat energy storage model

The heat energy is stored in a material at the hot site of the TEG. The specific heat capacity and the mass of the material (c_m and m_s, respectively). As the Q_h moved to the material, the T_h change with time, t. The heat energy storage model is based on (11), in which the new T_h, T_{h1}, is calculated [28].

$$T_{h1} = \int \frac{Q_m}{c_s m_s} dt + T_h \tag{11}$$

3. RESULTS AND DISCUSSIONS

The waveforms of the TEG ESS are shown in Figure 5. The voltage and current waveforms at the TEG array and DC bus are recorded to observe the flow of energy and the quality of the power produced. By referring to Figure 5(a), the V_{dc} is kept constant at 18 V. While the V_{teg} changes during charging and discharging. The voltage changes due to the characteristic of the TEG. During charging, the V_{teg} needs to be higher than V_{int} to ensure the charging occurs. The higher the ΔT, the higher the V_{teg} needed to transfer the energy to the TEG. The higher the P_{ref}, the higher the V_{teg}. During discharging, the V_{teg} needs to operate half of the V_{int}, which is the maximum power point. This is the reason why the V_{teg} is only around 5 V since the V_{int} is around 11 V. By referring to Figure 5(b), the I_{teg} and I_{bus} are positive and negative, respectively, and vice versa. Positive current represents the absorption of power and negative current represent the generation of power. During the charging cycle, the I_{teg} becomes positive and I_{bus} becomes negative. This is because the TEG array absorbs the power and DC bus supply the power.

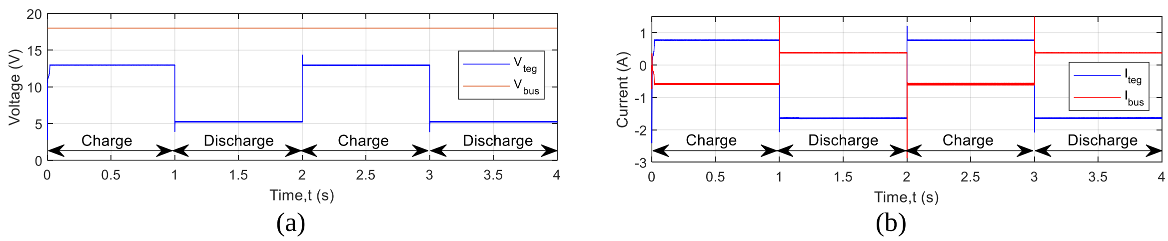

Figure 5. The voltage and current waveforms at the input and output of the bidirectional converter during charging and discharging for (a) the V_{teg} and V_{bus} against t and (b) the I_{teg} and I_{bus} against t

During discharging cycle, the I_{teg} becomes negative and I_{bus} becomes positive. This is because the TEG array supplies the power and the DC bus absorb the power. It is also observed that there is a larger current imbalance between I_{teg} and I_{bus} during discharging. This is due to the large voltage difference between V_{teg} and V_{bus}. Another important aspect observed is the voltage and current ripple. A good converter should have a low voltage and current ripple. The results show that the ripple is low. The is a slightly higher ripple on I_{bus} during charging. To improve the quality of the voltage and current, a proper design of the bidirectional converter for the TEG energy storage application should be implemented. Nonetheless, this design is currently unavailable. The design used is based on the try and error method only.

The power flow between the TEG array and DC bus is displayed in Figure 6(a). The positive power represents the absorption of power. While the negative power represents the supply of power. During the charging cycle, the P_{teg} becomes positive and P_{bus} becomes negative. This is because the TEG array absorbs the power and DC bus supply the power. During discharging cycle, the P_{teg} becomes negative and P_{bus} becomes positive. This is because the TEG array supplies the power and DC bus absorb the power. The dual flow of power during charging and discharging shows that the ESS based on TEG is feasible. Based on the powers, the efficiency (η) of the bidirectional converter is calculated and the result is shown in Figure 6(b). The result shows that the η is higher during charging compared to discharging. The η of the bidirectional converter is 95% and 79%, respectively. During charging, the bidirectional converter operates as the buck converter. The η of the buck converter is higher when the D is high. Since the D is high during charging, the efficiency of the bidirectional converter becomes high. During discharging, the bidirectional converter operates as the boost converter. The η of the boost converter is higher when the D is low. Since the D is high during discharging, the efficiency of the bidirectional converter becomes low.

Since the energy is stored in the form of heat at the hot site of the TEG array, the T_h changes during charging and discharging. During charging, the T_h of the heat energy storage increases, as shown in Figure 7. During discharging, the T_h of the heat energy storage decreases. Since the Th changes, this shows that the heat energy storage is capable of storing and releasing the energy from or to the TEG array.

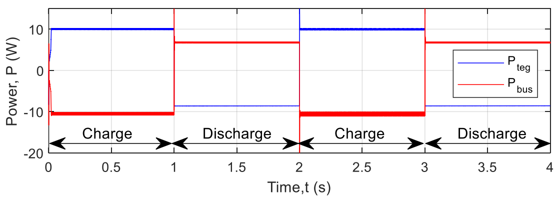

(a)

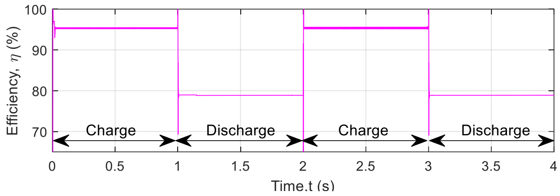

(b)

Figure 6. The power and efficiency of the TEG ESS during charging and discharging for (a) the P_{teg} and P_{bus} against time and (b) the η against time

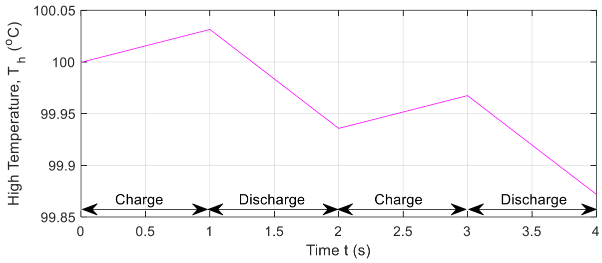

Figure 7. The T_h at the heat energy storage during charging and discharging, while the T_l is kept constant at 30 °C (environment)

Besides the input and output of the bidirectional converter, the operation of the bidirectional converter needs to be observed. This is to ensure the operation of the bidirectional converter is within the desired design specification. The D for the bidirectional converter needs to be between zero and one. If the D is out of the range, the system fails to operate and requires multiple adjustments at the design specifications. It is also important to keep the D 0.8 when the bidirectional converter operates in the boost mode, which is during discharging. This is because the bidirectional converter fails to operate after 0.8 if a closed-loop system is applied. The results in Figure 8(a) shows that the D is within the limit. However, the D is near 0.8 and the redesign is required to avoid fail operation. The ripple of the D also occurs since the fixed D_{step} is used in the control strategy. This can be improved by using a variable step size. Besides D, the continuous current mode is also the design specification of the ESS based on the TEG. The continuous current mode is observed using the L_m current, I_{Lm}, and the waveform is shown in Figure 8(b). The result shows that the I_{Lm} don't go to zero during the steady-state period for both charging and discharging conditions. This proves that the bidirectional converter operates in the continuous current mode operation.

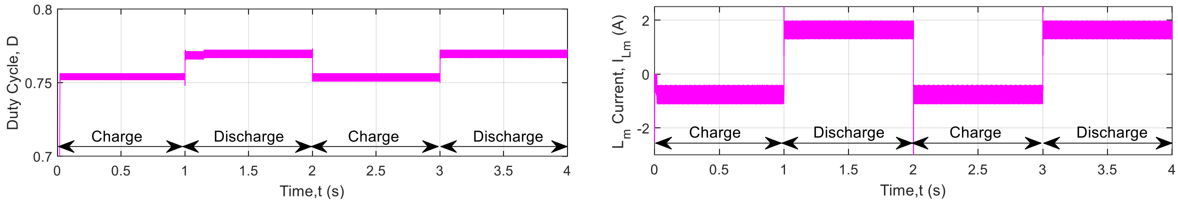

(a) (b)

Figure 8. The operation of the bidirectional converter for the TEG ESS during charging and discharging for (a) the *D* against *t* and (b) the I_{Lm} against *t*

4. CONCLUSION

The objective of the paper is to propose a design and determine the possibility of using TEG technology as energy storage. The system uses a bidirectional converter to exchange energy between the DC bus and heat energy storage using the TEG array and bidirectional converter. The results show that the heat and electrical energies can be exchange between the DC bus and heat energy storage. The quality of the voltage and current is also observed to ensure the energy exchange is usable. The result shows that the absorb or supply power quality has a low ripple. In conclusion, energy storage based on TEG is feasible. Nonetheless, there is still further improvement that needs to be made. This includes the design of the component of the bidirectional controller and the improved control strategy.

ACKNOWLEDGEMENTS

This research was supported by Ministry of Higher Education (MOHE) through Fundamental Research Grant Scheme (FRGS/1/2021/TK0/UTM/02/19). The authors would like to express gratitude to Universiti Teknologi Malaysia (UTM) for providing comprehensive facilities. Lastly, thanks to colleagues who have either directly or indirectly contributed to the completion of this work.

REFERENCES

[1] REN21, "Renewables 2021 global status report (GSR)," REN21 Renewables Now, 2021, [Online]. Available: https://www.ren21.net/gsr-2021/. (accessed Jun. 06, 2022)
[2] M. M. Rahman, A. O. Oni, E. Gemechu, and A. Kumar, "Assessment of energy storage technologies: a review," *Energy Conversion and Management*, vol. 223, p. 113295, Nov. 2020, doi: 10.1016/j.enconman.2020.113295.
[3] S. Koohi-Fayegh and M. A. Rosen, "A review of energy storage types, applications and recent developments," *Journal of Energy Storage*, vol. 27, p. 101047, Feb. 2020, doi: 10.1016/j.est.2019.101047.
[4] A. Olabi, C. Onumaegbu, T. Wilberforce, M. Ramadan, M. A. Abdelkareem, and A. H. Al–Alami, "Critical review of energy storage systems," *Energy*, vol. 214, p. 118987, Jan. 2021, doi: 10.1016/j.energy.2020.118987.
[5] J. D. Hunt *et al*., "Existing and new arrangements of pumped-hydro storage plants," *Renewable and Sustainable Energy Reviews*, vol. 129, p. 109914, Sep. 2020, doi: 10.1016/j.rser.2020.109914.
[6] I. Rais and H. Mahmoudi, "The dimensioning of a compressed air motor dedicated to a compressed air storage system," *International Journal of Power Electronics and Drive Systems (IJPEDS)*, vol. 9, no. 1, pp. 73-79, Mar. 2018, doi: 10.11591/ijpeds.v9.i1.pp73-79.
[7] B. Amel, Z. Soraya, and C. Abdelkader, "RT-lab based real-time simulation of flywheel energy storage system associated to a variable-speed wind generator," *International Journal of Power Electronics and Drive Systems (IJPEDS)*, vol. 12, no. 2, pp. 1094-1101, Jun. 2021, doi: 10.11591/ijpeds.v12.i2.pp1094-1101.
[8] B. V. Rajanna and M. K. Kumar, "Comparison study of lead-acid and lithium-ıon batteries for solar photovoltaic applications," *International Journal of Power Electronics and Drive Systems (IJPEDS)*, vol. 12, no. 2, pp. 1069-1082, Jun. 2021, doi: 10.11591/ijpeds.v12.i2.pp1069-1082.
[9] W. Punin, S. Maneewan, and C. Punlek, "Thermoelectric generator for the recovery of energy from the low-grade heat sources in sugar industry," *International Journal of Power Electronics and Drive Systems (IJPEDS)*, vol. 9, no. 4, pp. 1565-1572, Dec. 2018, doi: 10.11591/ijpeds.v9.i4.pp1565-1572.
[10] H. Jouhara *et al*., "Thermoelectric generator (TEG) technologies and applications," *International Journal of Thermofluids*, vol. 9, p. 100063, Feb. 2021, doi: https: 10.1016/j.ijft.2021.100063.
[11] X. Wen, J. Ji, Z. Song, Z. Li, H. Xie, and J. Wang, "Comparison analysis of two different concentrated photovoltaic/thermal-TEG hybrid systems," *Energy Conversion and Management*, vol. 234, p. 113940, Apr. 2021, doi: 10.1016/j.enconman.2021.113940.
[12] H. Zhang, H. Yue, J. Huang, K. Liang, and H. Chen, "Experimental studies on a low concentrating photovoltaic/thermal (LCPV/T) collector with a thermoelectric generator (TEG) module," *Renewable Energy*, vol. 171, pp. 1026-1040, Jun. 2021, doi: https: 10.1016/j.renene.2021.02.133.
[13] K. Karthick, S. Suresh, G. C. Joy, and R. Dhanuskodi, "Experimental investigation of solar reversible power generation in thermoelectric generator (TEG) using thermal energy storage," *Energy for Sustainable Development*, vol. 48, pp. 107-114, Feb. 2019, doi: 10.1016/j.esd.2018.11.002.

[14] X. Sui, W. Li, Y. Zhang, and Y. Wu, "Theoretical and experimental evaluation of a thermoelectric generator using concentration and thermal energy storage," in *IEEE Access*, vol. 8, pp. 87820-87828, 2020, doi: 10.1109/ACCESS.2020.2993288.
[15] K. Huang, Y. Yan, G. Wang, and B. Li, "Improving transient performance of thermoelectric generator by integrating phase change material," *Energy*, vol. 219, p. 119648, Mar. 2021, doi: 10.1016/j.energy.2020.119648.
[16] N. P. Bayendang, M. T. E. Kahn, V. Balyan, I. Draganov, and S. Pasupathi, "A comprehensive thermoelectric generator (TEG) modelling," in *AIUE Proceedings of the Energy and Human Habitat Conference 2020*, Nov. 2020, doi: 10.5281/zenodo.4289574.
[17] S. Singh, O. I. Ibeagwu, and R. Lamba, "Thermodynamic evaluation of irreversibility and optimum performance of a concentrated PV-TEG cogenerated hybrid system," *Solar Energy*, vol. 170, pp. 896-905, Aug. 2018, doi: 10.1016/j.solener.2018.06.034.
[18] R. Ayop, C. W. Tan, and C. S. Lim, "The resistance comparison method using integral controller for photovoltaic emulator," *International Journal of Power Electronics and Drive Systems (IJPEDS)*, vol. 9, no. 2, pp. 820-828, Jun. 2018, doi: 10.11591/ijpeds.v9.i2.pp820-828.
[19] R. Ayop, S. M. Ayob, C. W. Tan, T. Sutikno, and M. J. A. Aziz, "Comparison of electronic load using linear regulator and boost converter," *International Journal of Power Electronics and Drives (IJPEDS)*, vol. 12, no. 3, pp. 1720-1728, 2021, doi: 10.11591/ijpeds.v12.i3.pp1720-1728.
[20] D. W. Hart, *Power Electronics*, New York, USA: Tata McGraw-Hill Education, 2011.
[21] A. Belkaid, I. Colak, K. Kayisli, R. Bayindir, and H. I. Bulbul, "Maximum power extraction from a photovoltaic panel and a thermoelectric generator constituting a hybrid electrical generation system," *2018 International Conference on Smart Grid (icSmartGrid)*, 2018, pp. 276-282, doi: 10.1109/ISGWCP.2018.8634534.
[22] I. Laird and D. D. C. Lu, "Steady state reliability of maximum power point tracking algorithms used with a thermoelectric generator," in *2013 IEEE International Symposium on Circuits and Systems (ISCAS)*, 2013, pp. 1316-1319, doi: 10.1109/ISCAS.2013.6572096.
[23] R. Ayop and C. W. Tan, "An adaptive controller for photovoltaic emulator using artificial neural network," *Indonesian Journal of Electrical Engineering and Computer Science*, vol. 5, no. 3, pp. 556-563, Mar. 2017, doi: 10.11591/ijeecs.v5.i3.pp556-563.
[24] H. Attia and S. Ulusoy, "A new perturb and observe MPPT algorithm based on two steps variable voltage control," *International Journal of Power Electronics and Drive Systems (IJPEDS)*, vol. 12, no. 4, pp. 2201-2208, Dec. 2021, doi: http: 10.11591/ijpeds.v12.i4.pp2201-2208.
[25] T. H. Kwan and X. Wu, "High performance P&O based lock-on mechanism MPPT algorithm with smooth tracking," *Solar Energy*, vol. 155, pp. 816-828, Oct. 2017, doi: 10.1016/j.solener.2017.07.026.
[26] R. Balasankar, G. T. Arasu, and J. S. C. M. Raj, "A global MPPT technique invoking partitioned estimation and strategic deployment of P&O to tackle partial shading conditions," *Solar Energy*, vol. 143, pp. 73-85, 2017, doi: 10.1016/j.solener.2016.12.018.
[27] J. Gao *et al*., "A thermoelectric generation system and its power electronics stage," *Journal of Electronic Materials*, vol. 41, no. 6, pp. 1043-1050, 2012, doi: 10.1007/s11664-012-2034-5.
[28] J. Khachan, "Summary of equations", in *Thermal Properties of Matter*, San Rafael CA, USA: Morgan & Claypool Publishers, 2018, doi: 10.1088/978-1-6817-4585-5ch7.

BIOGRAPHIES OF AUTHORS

Razman Ayop received the bachelor's degree in electrical engineering with first-class honours, the master's degree in electrical engineering with specialization in power system, and the Ph.D. degree in electrical engineering from Universiti Teknologi Malaysia (UTM), Johor, Malaysia, in 2013, 2015, and 2018, respectively. He is a Senior Lecturer with UTM and a member of Power Electronics and Drives Research Group, School of Electrical Engineering, Faculty of Engineering, UTM. His research interests include renewable energy and power electronics. He can be contacted at email: razman.ayop@utm.my.

Chee Wei Tan received his B.Eng. degree in Electrical Engineering (First Class Honors) from Universiti Teknologi Malaysia (UTM), in 2003 and a Ph.D. degree in Electrical Engineering from Imperial College London, London, U.K., in 2008. He is currently an associate professor at Universiti Teknologi Malaysia and a member of the Power Electronics and Drives Research Group, School of Electrical Engineering, Faculty of Engineering. His research interests include the application of power electronics in renewable/alternative energy systems, control of power electronics and energy management system in microgrids. He can be contacted at email: cheewei@utm.my.

Abba Lawan Bukar is a lecturer at the Department of Electrical and Electronic Engineering, University of Maiduguri. His research interest includes renewable energy technologies, energy management optimization. He can be contacted at email: abbalawan9@gmail.com.

Awang Jusoh was born in Terengganu, Malaysia in 1964. He received his B. Eng. (Hons) from Brighton Polytechnic, UK, in 1988. He obtained his MSc. and Ph.D. from The University of Birmingham, UK in 1995 and 2004, respectively. Since 1989, he has been a lecturer at Universiti Teknologi Malaysia and is now an Associate Professor at the Department of Power Engineering, School of Electrical Engineering, Faculty of Engineering, Universiti Teknologi Malaysia, Malaysia. His research interests include all areas of power electronics systems and renewable energy. He can be contacted at email: awang@utm.my.

Nik Din Muhamad is a lecturer at the Universiti Teknologi Malaysia, Johor, Malaysia since 1989 and the director of the Electrical Machine Laboratory there. His research focuses on modeling, design and control of DC-DC converters. He earned a B. Eng from Universiti Teknologi Malaysia and and M. Eng in electrical engineering from the same university. He can be contacted at email: nikd@utm.my.

Syed Norazizul Syed Nasir received the B.Eng. (Hons) degree in electrical engineering in 2008, M.Eng. degree in electrical (power) engineering in 2014 and Ph.D. degree in electrical (power) engineering in 2019 from Universiti Teknologi Malaysia (UTM), Johor Bahru, Malaysia. He works as Electrical Engineer in high voltage protection since 2008 until 2019 at Tenaga Nasional Berhad. He is currently senior lecturer in School of Electrical Engineering at Universiti Teknologi Malaysia (UTM). His current research interests include power system optimization, power system stability, power system protection and harmonic mitigation and their control methods. He can be contacted at email: syednorazizul@utm.my.